Available online at www.sciencedirect.com
SCIENCE DIRECT®
Journal of Chromatography A, 1079 (2005) 92–104
JOURNAL OF CHROMATOGRAPHY A
www.elsevier.com/locate/chroma

Effect of charge regulation on steric mass-action equilibrium for the ion-exchange adsorption of proteins

Hong Shen, Douglas D. Frey *

Department of Chemical and Biochemical Engineering, University of Maryland Baltimore County, 1000 Hilltop Circle, Baltimore, MD 21250, USA

Available online 7 April 2005

Abstract

A thermodynamic formalism is developed for incorporating the effects of charge regulation on the ion-exchange adsorption of proteins under mass-overloaded conditions as described by the steric mass-action (SMA) isotherm. To accomplish this, the pH titration behavior of a protein and the associated adsorption equilibrium of the various charged forms of a protein are incorporated into a model which also accounts for the steric hindrance of salt counterions caused by protein adsorption. For the case where the protein is dilute, the new model reduces to the protein adsorption model described recently by the authors which accounts for charge regulation. Similarly, the new model reduces to the steric mass-action isotherm developed by Brooks and Cramer which applies to mass-overloaded conditions for the case where charge regulation is ignored so that the protein has a fixed charge. Calculations using the new model were found to agree with experimental data for the adsorption of bovine serum albumin (BSA) on an anion-exchange column packing when using reasonable physical properties. The new model was also used to develop an improved theoretical criterion for determining the conditions required for an adsorbed species to displace a protein in displacement chromatography when the pH is near the protein p*I*.

Keywords: Ion-exchange equilibrium; Protein adsorption; Displacement chromatography; Steric mass-action isotherm

1. Introduction

Most models for protein ion-exchange adsorption described previously in the literature assume that the adsorbed protein exists in a single charge state during the entire adsorption process [1–7]. However, it is well known that when a polyelectrolyte approaches a charged surface, the net charge on the polyelectrolyte is influenced by the electrostatic field produced by the surface [8–12]. An early attempt to account for this phenomenon, often termed "charge regulation," was made by Sluyterman and Elgersma [13] who envisioned the adsorbed phase as being uniform in composition so that the macroscopic laws of thermodynamics could be used to describe the effect of the different hydrogen ion concentrations in the fluid and adsorbed phases on the protein charge state. More recently, Ståhlberg and Jönsson [14] developed a colloidal model for charge regulation of a dilute protein based on a microscopic description in which the adsorbed phase is represented as an electric double layer, and the Poisson–Boltzmann equation used to account for the electrostatic effect produced by the adsorbent on the charge state of the protein. However, in addition to being restricted to dilute proteins, both of these models contain other approximations that limit their use in practice. For example, although the model of Ståhlberg and Jönsson is a very important advance in the modeling of charge regulation, its accuracy is limited when the fluid-phase pH is near the protein p*I*, which is often the case of most interest when considering charge regulation.

Recently, Shen and Frey [15] extended the approach of Sluyterman and Elgersma [13] in order to develop a multiple charge state (MCS) model that is an improved theoretical description of the ion-exchange adsorption of a dilute protein which accounts for charge regulation. Shen and Frey also demonstrated that by accounting for charge regulation, the net protein charge in the fluid phase used in their model is significantly closer to the actual protein charge in the fluid

* Corresponding author. Tel.: +1 410 455 3418; fax: +1 410 455 6500.
E-mail address: dfrey1@umbc.edu (D.D. Frey).

0021-9673/$ – see front matter © 2005 Elsevier B.V. All rights reserved.
doi:10.1016/j.chroma.2005.02.086

phase, as compared to the characteristic binding charge in the traditional stoichiometric displacement model [1]. In the present study, the approach of Shen and Frey is extended to the case of mass overloading where steric hindrance of salt counterions is caused by protein adsorption. The resulting model can therefore be considered not only an extension of the MCS model to the case of protein mass overloading, but also an extension of the steric mass-action (SMA) adsorption isotherm to the case where protein charge regulation is accounted for. Although other extensions of the SMA adsorption isotherm exist, such as the extension to the case of thermodynamically nonideal mixtures by Raje and Pinto [7,16], and the extension to the case of variable pH by Bosma and Wesselingh [17,18], none of these previous extensions incorporate the effects of protein charge regulation.

The concept of SMA equilibrium for ion-exchange adsorption, in which it is recognized that only a fraction of the functional groups on the adsorbent surface underneath an adsorbed protein interact directly with the protein, was first described by Velayudhan [19], formerly at Oregon State University and currently at Bristol-Myers Squibb, whose doctoral thesis mentor was Csaba Horváth. Steven Cramer, who is currently at Rensselaer Polytechnic Institute and whose doctoral thesis mentor was also Csaba Horváth, subsequently translated the concept of SMA equilibrium into precise mathematical terms in collaboration with several co-workers [6]. Extensions of the SMA formalism, particularly extensions relevant to the implementation of displacement chromatography as discussed in this study, are therefore appropriate topics for recognizing not only the seminal contributions of Csaba Horváth in the field of chromatography, but also his mentorship of leading industrial and academic scientists in this field.

2. Theory

2.1. General considerations

In this study, the adsorbed phase is assumed to be uniform in composition so that standard thermodynamic relations describing phase equilibrium between two bulk phases can be applied [20–24]. In addition, the ionogenic functional groups on the protein are assumed to ionize according to acid–base equilibrium constants that remain fixed and independent of the protein charge. The charge state of the protein in the fluid phase is therefore assumed to be determined by the local pH in that phase, and the change in protein charge caused by adsorption is assumed to be determined by the tendency of the more highly charged forms of the protein to interact electrostatically with the adsorbent to a greater degree than lesser charged forms of the protein. Equivalently, the change in protein charge caused by adsorption can be envisioned as resulting from the difference in the hydrogen ion concentrations in the fluid and adsorbed phases, and from the corresponding

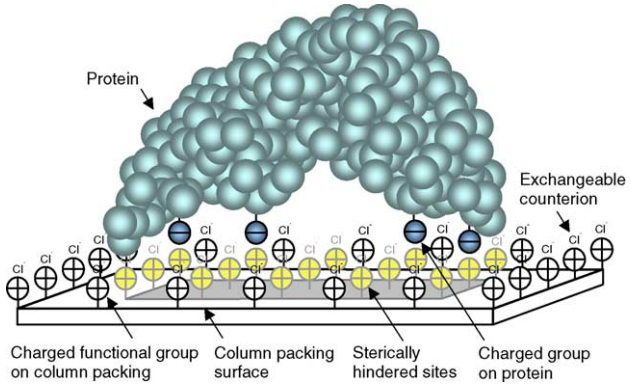

Fig. 1. Illustration of a protein having four negatively charged groups which interact with four positively charged groups on the column packing. The chloride counterion forms undissociated ion pairs with the sites underneath the protein in the gray area, while the chloride ion is an exchangeable counterion outside the gray area. The total number of functional groups on the column packing within the gray area is the steric factor σ.

hydrogen ion titration behavior of the protein in those two phases.

As shown in Fig. 1, the total number of adsorption sites underneath a protein adsorbed onto a charged surface is larger than the number of adsorption sites that interact directly with the protein, in which case a significant number of salt counterions are sterically hindered from participating in ion-exchange equilibrium. Steric effects of this type are particularly important to account for under mass-overloaded conditions since the saturation adsorption capacity of an adsorbent is determined by the area occupied by the protein on the surface, as reflected by the total number of adsorption sites underneath the protein.

Since the steric effect illustrated in Fig. 1 is a consequence of the colloidal nature of the adsorption process, it cannot be accounted for by a description of adsorption equilibrium based solely on equating the chemical potentials of particular species in three-dimensional fluid and adsorbed phases unless extra-thermodynamic relations are employed. Such an approach is commonly used, among other applications, in so-called “chemical” thermodynamic theories for predicting activity coefficients where intermolecular interactions are represented by chemical reactions that form new species [25]. In order to ensure that the new adsorption equilibrium model developed here reduces asymptotically to the traditional SMA isotherm when the adsorbed protein has a fixed charge, the model will employ the same extra-thermodynamic relation used by Brooks and Cramer [6] to develop that isotherm. As shown below, this extra-thermodynamic relation corresponds to the assumption that, with regard to their role in protein adsorption equilibrium, sterically hindered adsorption sites and their associated counterions function thermodynamically as if the adsorption site and counterion form undissociated ion pairs, in which case the adsorbed phase is envisioned as a uniform mixture of these ion pairs, salt counterions, proteins, hydrogen and hydroxide ions, and the adsorbent functional groups. Furthermore, it was effectively assumed by Brooks

and Cramer that adsorbed proteins are sufficiently mobile diffusionally so that the activity of the exchangeable counterions is proportional to the number of these ions per unit volume of the entire adsorbed phase, including the volume occupied by the sterically hindered sites. Although these particular assumptions could be questioned on the basis of whether they properly reflect the true colloidal nature of the adsorption process, the use of these assumptions does yield a thermodynamically consistent adsorption model which asymptotically approaches the traditional SMA isotherm in the limit where the protein has a fixed charge, which is sufficient justification for employing these assumptions in the present case.

Although the study of Shen and Frey [15] addressed the case of charge regulation for a dilute protein, the key relation in their model between the protein equilibrium distribution coefficient and the Donnan potential applies whether or not the protein is dilute provided that the only interaction between adsorbed proteins is the steric interaction which prevents proteins of finite size from physically overlapping. Consequently, as demonstrated below, the relations accounting for charge regulation developed by Shen and Frey can be extended in a straightforward way to the case of mass overloading by accounting for the effects of steric hindrance of salt counterions on the Donnan potential using the assumptions just described. In this way, a result can be developed that approaches asymptotically the model of Shen and Frey in the limit of low protein concentrations and, as mentioned above, which also approaches asymptotically the SMA model in the limit where charge regulation is negligible. Since there is considerable experimental evidence that the two models just mentioned describe protein adsorption behavior accurately in their applicable regimes [6,15], it is likely that the new adsorption model developed in this study will be a useful description of protein adsorption behavior which is more general than previous such descriptions in the literature.

2.2. Adsorption of a single protein having a single charged state of $-m$

Consider first the simple case addressed originally by Brooks and Cramer [6] where a protein having a fixed charge of $-m$, where m is a positive number, adsorbs onto an anion-exchange column packing, and where the adsorbed phase is assumed to be uniform in composition. Assuming also for illustrative purposes the case where the chloride ion is the counterion, adsorption equilibrium can be expressed using the following relation [6]:

$$q_{\mathrm{P}^{-m}} = K_{\mathrm{eq,P}} C_{\mathrm{P}^{-m}} \left(\frac{q_{\mathrm{Cl}^-,\mathrm{a}}}{C_{\mathrm{Cl}^-}} \right)^m \tag{1}$$

where $q_{\mathrm{P}^{-m}}$ is the equilibrium amount of protein per unit volume of the adsorbed phase and $q_{\mathrm{Cl}^-,\mathrm{a}}$ is the equilibrium amount of exchangeable counterion per unit volume of the adsorbed phase. Eq. (1) is the starting point used by Brooks and Cramer to develop the traditional SMA isotherm. This equation is also equivalent to the relation used in the MCS model of Shen and Frey [15] to represent adsorption equilibrium, except that in this previous model it was assumed that the protein is dilute so that $q_{\mathrm{Cl}^-,\mathrm{a}} = q_{\mathrm{Cl}^-}$, and equilibrium was written in terms of the ratio of the hydrogen ion concentrations in the fluid and adsorbed phases, instead of the ratio of counterion concentrations. Note that equilibrium concentrations were denoted with the superscript * in the previous work just mentioned, while in the present study this subscript has been deleted from the equilibrium concentrations. The parameter $K_{\mathrm{eq,P}}$ used in Eq. (1) is the ion-exchange equilibrium constant, which is equivalent to the quantity $K_{\mathrm{P,ads}}/(K^m_{\mathrm{Cl}^-,\mathrm{ads}})$ used by Shen and Frey, where $K_{\mathrm{Cl}^-,\mathrm{ads}}$ is the adsorption equilibrium constant for HCl (see Eq. (10)) and $K_{\mathrm{P,ads}}$ is the same quantity for the protein. Furthermore, if thermodynamic ideality is assumed for the H^+ and Cl^- ions, then $K_{\mathrm{Cl}^-,\mathrm{ads}} = 1$, and $K_{\mathrm{eq,P}}$ in Eq. (1) is numerically equal to $K_{\mathrm{P,ads}}$ as used in the MCS model of Shen and Frey.

As shown in Fig. 1, when a protein adsorbs onto a charged surface, a certain number of adsorption sites are sterically hindered from participating in ion-exchange equilibrium by the presence of the protein. It is assumed here, as in the original SMA isotherm model of Brooks and Cramer, that these blocked sites behave with regard to their effect on protein adsorption as undissociated ion pairs so that, although they occupy space in the adsorbed phase, their presence does not contribute to the activity of the counterions in that phase. The concentration of counterions available for participating in ion-exchange equilibrium, denoted as $q_{\mathrm{Cl}^-,\mathrm{a}}$ in Eq. (1), is consequently given by

$$q_{\mathrm{Cl}^-,\mathrm{a}} = q_{\mathrm{Cl}^-} - (\sigma - m) q_{\mathrm{P}^{-m}} \tag{2}$$

where q_{Cl^-} is the total counterion concentration in the adsorbed phase, and σ is the total number of sites underneath the protein.

If the concentrations of H^+ and OH^- ions in the adsorbed phase are assumed to be small, and if the effect of co-ion uptake is ignored as described previously [15], then the electroneutrality condition in the adsorbed phase can be expressed as:

$$q_{\mathrm{R}^+} = q_{\mathrm{Cl}^-} + m q_{\mathrm{P}^{-m}} \tag{3}$$

where q_{R^+} is the concentration of ion-exchange functional groups in the charged form. If furthermore an effective dimensionless Donnan potential, ϕ', is defined to be $\ln(q_{\mathrm{Cl}^-,\mathrm{a}}/C_{\mathrm{Cl}^-})$, and if $K_{\mathrm{Cl}^-,\mathrm{ads}} = 1$, then Eqs. (2) and (3) can be combined to yield

$$\phi' = \ln\left(\frac{q_{\mathrm{R}^+} - q_{\mathrm{P}^{-m}}\sigma}{C_{\mathrm{Cl}^-}} \right) \tag{4}$$

Note that ϕ' represents the electrical potential energy difference between the fluid and adsorbed phases corrected for the steric effect. It therefore differs from the actual effective dimensionless Donnan potential given by $\ln(q_{\mathrm{Cl}^-}/C_{\mathrm{Cl}^-})$ or, as in the MCS model of Shen and Frey [15], by $\ln(C_{\mathrm{H}^+}/q_{\mathrm{H}^+})$,

depending on whether Cl^- or H^+ is selected as the so-called potential determining ion [21,24]. Combining Eqs. (1)–(3) yields

$$C_{P^{-m}} = \frac{q_{P^{-m}}}{K_{eq,P}} \left(\frac{C_{Cl^-}}{q_{R^+} - \sigma q_{P^{-m}}} \right)^m \quad (5)$$

which is equivalent to the SMA isotherm developed by Brooks and Cramer [6] except for the different definition for the steric factor, i.e., $\sigma = \sigma_{BC} + m$, where σ_{BC} denotes the steric factor used by Brooks and Cramer.

2.3. Effective dimensionless Donnan potential for the case of a single adsorbed protein having the three charge states −m, 0, and m

As discussed above, the relation between the protein adsorption distribution coefficient and the Donnan potential developed by Shen and Frey [15] which accounts for charge regulation can be incorporated into the SMA isotherm model provided that the Donnan potential used accounts for steric effects by being consistent with the extra-thermodynamic assumption used by Brooks and Cramer [6]. For this purpose, as discussed by Shen and Frey, it is convenient to approximate acid–base equilibrium for a protein having a total of n charged states that are equally distributed around the state of zero charge by assuming that the only charged states that exist are the $-m$, 0, and m states where $2m + 1 = n$, and where the average charge on the protein is the mole fraction weighted average of the $-m$, 0 and m charged states. Acid–base equilibrium for the protein can consequently be written as

$$P^m \leftrightarrow P^0 + mH^+ \leftrightarrow P^{-m} + 2mH^+ \quad (6)$$

while adsorption equilibrium for the three charged forms of the protein and for the chloride ion can be expressed as

$$q_{P^{-m}} = K_{eq,P} C_{P^{-m}} (\exp(\phi'))^m \quad (7)$$

$$q_{P^0} = K_{eq,P} C_{P^0} (\exp(\phi'))^0 \quad (8)$$

$$q_{P^m} = K_{eq,P} C_{P^m} (\exp(\phi'))^{-m} \quad (9)$$

$$q_{Cl^-,a} q_{H^+} = K_{Cl^-,ads} C_{Cl^-} C_{H^+} \quad (10)$$

where ϕ' is the effective dimensionless Donnan potential given by $\ln(q_{Cl^-,a}/C_{Cl^-})$. Eqs. (7)–(9) are equivalent to the relations used by Shen and Frey [15] in the limit where the protein is dilute so that $\phi' \to \phi$. Note that Eq. (9) describes the electrostatic repulsion of the positively charged form of the protein from the positively charged surface of the anion-exchange adsorbent, and that $K_{eq,P}$ in Eqs. (7)–(9) is equivalent to the quantity $K_{P,ads}$ as used by Shen and Frey since it is assumed in the above equations, as well as in all the following equations, that $K_{Cl^-,ads} = 1$. Note finally that the total concentration of adsorbed protein, q_P, is given by the sum $q_{P^{-m}} + q_{P^0} + q_{P^m}$, and that the isoelectric point of the protein is the same in the fluid and adsorbed phases since the adsorption equilibrium constants for all the charged forms are equal [15].

The model just described can be extended in a number of ways that in certain cases may increase its usefulness for describing protein adsorption. For example, the charge distribution can be centered around a non-zero charge state, more than three charge states can be accounted for, and the adsorption equilibrium constants can differ among the various charge states. This last extension accounts for a change in the isoelectric point caused by adsorption, which has been reported in some cases for the ion-exchange adsorption of amino acids [26]. Although these various extensions may be useful under some conditions, it is shown in Section 3.3 that the simplest version of the model not including these extensions is able to fit experimental data for protein adsorption with reasonable accuracy.

Assuming again for illustrative purposes the case of an anion-exchange adsorbent, and assuming also that the m counterions associated with the positively charged form of the protein do not participate in ion-exchange equilibrium with other proteins, then the concentration of adsorbed counterions available for participation in ion-exchange equilibrium can be expressed as

$$q_{Cl^-,a} = q_{Cl^-} - (\sigma - m) q_{P^{-m}} - \sigma q_{P^0} - (\sigma + m) q_{P^m} \quad (11)$$

The electroneutrality condition in the adsorbed phase is given by

$$q_{R^+} = q_{Cl^-} - m q_{P^m} + m q_{P^{-m}} \quad (12)$$

If Eqs. (11) and (12) are combined, the result is the following equation which is formally similar to Eq. (4), but which relates the effective dimensionless Donnan potential to the composition of the adsorbed phase for the case of a single adsorbed protein having the three charge states of $-m$, 0, and m:

$$\phi' = \ln \left(\frac{q_{R^+} - q_P \sigma}{C_{Cl^-}} \right) \quad (13)$$

2.4. Effective dimensionless Donnan potential for the case of several proteins each having the three charge states −m_i, 0, and m_i

The development in Section 2.3 can be extended to the case where any number of adsorbed proteins exist. In particular, adsorption equilibrium for the jth charge state of protein i can be expressed as:

$$q_{i,j} = K_{eq,i} C_{i,j} (\exp(\phi'))^{-z_{i,j}} \quad (14)$$

The concentration of counterions available for participating in ion-exchange equilibrium can then be expressed as:

$$q_{Cl^-,a} = q_{Cl^-} - \sum_i \sum_j (\sigma_i + z_{i,j}) q_{i,j} \quad (15)$$

By defining the average charge of the proteins in the adsorbed phase, z_{ave}, as

$$z_{ave} = \sum_i \sum_j \frac{z_{i,j} q_{i,j}}{q_P} \tag{16}$$

where $q_P = \sum_i \sum_j q_{i,j}$, then Eq. (15) can be written as

$$q_{Cl^-,a} = q_{Cl^-} - \left(\sum_i \frac{\sigma_i q_i}{q_P} + z_{ave} \right) q_P \tag{17}$$

where $q_i = \sum_j q_{i,j}$. The electroneutrality condition in the adsorbed phase can then be expressed as:

$$q_{R^+} = q_{Cl^-} - z_{ave} q_P \tag{18}$$

If Eqs. (17) and (18) are combined, the result is the following equation which, like Eq. (13), is formally similar to Eq. (4), but which relates the effective dimensionless Donnan potential to the composition of the adsorbed phase for the case of several proteins, each of which possess the three charge states of $-m_i$, 0, and m_i:

$$\phi' = \ln \left(\frac{q_{R^+} - \sum_i \sigma_i q_i}{C_{Cl^-}} \right) \tag{19}$$

2.5. Protein adsorption equilibrium under mass-overloaded conditions

Consider first the case of a weak-base anion-exchange adsorbent having a single functional group R with a concentration of q_R. If the acid–base equilibrium constant for this functional group is denoted as K_R, then the equilibrium relation describing the ionization of this functional group in the adsorbed phase can be written as

$$q_{R^+} = \frac{q_{H^+} q_R}{K_R + q_{H^+}} \tag{20}$$

Since $\mathrm{pH} = -\log(C_{H^+})$ and $\mathrm{p}K_R = -\log(K_R)$, Eqs. (10), (13) and (20) can be combined to yield

$$q_P = \frac{10^{\mathrm{p}K_R}(q_R - C_{Cl^-} \exp(\phi')) - 10^{\mathrm{pH}} C_{Cl^-} \exp(2\phi')}{\sigma(10^{\mathrm{pH}} \exp(\phi') + 10^{\mathrm{p}K_R})} \tag{21}$$

If a single protein having the charged states $-m$, 0 and m is the adsorbate, and if adsorption equilibrium for each of these charge states is described by a Boltzmann distribution as given by Eqs. (7)–(9), then it was shown by Shen and Frey [15] that the distribution coefficient for the protein, K_d, defined as the ratio of the total of the individual protein forms in the adsorbed phase per unit volume to the same quantity in the fluid phase, can be expressed as

$$K_d = K_{P,ads} \exp(m\phi') \left[\frac{(dz/dpH)_{pI}(1 - 10^{m(pI-pH)} \exp(-m\phi'))^2 - 2 \ln(10) m^2 10^{m(pI-pH)} \exp(-m\phi')}{(dz/dpH)_{pI}(1 - 10^{m(pI-pH)})^2 - 2 \ln(10) m^2 10^{m(pI-pH)}} \right] \tag{22}$$

where the pH used in the equation is that for the fluid phase and $(dz/dpH)_{pI}$ is the change in the protein charge with pH at the protein pI. Since $K_d = q_P/C_P$, Eqs. (21) and (22) can be combined to eliminate q_P so that a single implicit equation for the Donnan potential results. The solution of this equation for specific values of C_P, pH, and C_{Cl^-} can then be substituted into Eq. (22) so that this equation can be used to calculate the corresponding value of q_P. Repeating this procedure for other values of C_P, pH, and C_{Cl^-} yields the adsorption isotherm for the case of a single protein under mass-overloaded conditions where the protein can potentially exist in either of the three charged states $-m$, 0, and m, and where the protein charge state is determined by the local environment in the fluid and adsorbed phases. Finally, for the simplified case of a strong-base anion-exchange adsorbent, q_{R^+} is specified so that Eqs. (13) and (22) directly provide an implicit relation between q_P and C_P which defines the adsorption isotherm.

Although an anion-exchange adsorbent was considered in the development just given, Eq. (22) applies as well to a cation-exchange adsorbent. For this latter case, the effective dimensionless Donnan potential, ϕ', is a negative number, and Eq. (22) is more conveniently written in the following alternative form:

$$K_d = K_{P,ads} \exp(-m\phi') \left[\frac{(dz/dpH)_{pI}(\exp(m\phi') - 10^{m(pI-pH)})^2 - 2 \ln(10) m^2 10^{m(pI-pH)} \exp(m\phi')}{(dz/dpH)_{pI}(1 - 10^{m(pI-pH)})^2 - 2 \ln(10) m^2 10^{m(pI-pH)}} \right] \tag{23}$$

where m is still taken as a positive number.

For a multicomponent mixture of proteins where the ith protein has the charged forms of $-m_i$, 0 and m_i, the distribution coefficient, $K_{d,i}$, for this protein can be expressed in a form similar to Eq. (22):

$$K_{d,i} = K_{i,ads} \exp(m_i\phi') \left[\frac{(dz/dpH)_{pI_i}(1 - 10^{m_i(pI_i-pH)} \exp(-m_i\phi'))^2 - 2 \ln(10) m_i^2 10^{m_i(pI_i-pH)} \exp(-m_i\phi')}{(dz/dpH)_{pI_i}(1 - 10^{m_i(pI_i-pH)})^2 - 2 \ln(10) m_i^2 10^{m_i(pI_i-pH)}} \right] \tag{24}$$

Consider first the case of a strong-base anion-exchange adsorbent where the total number of proteins present is $n_{protein}$. Under these conditions, Eqs. (19) and (24) provide a system

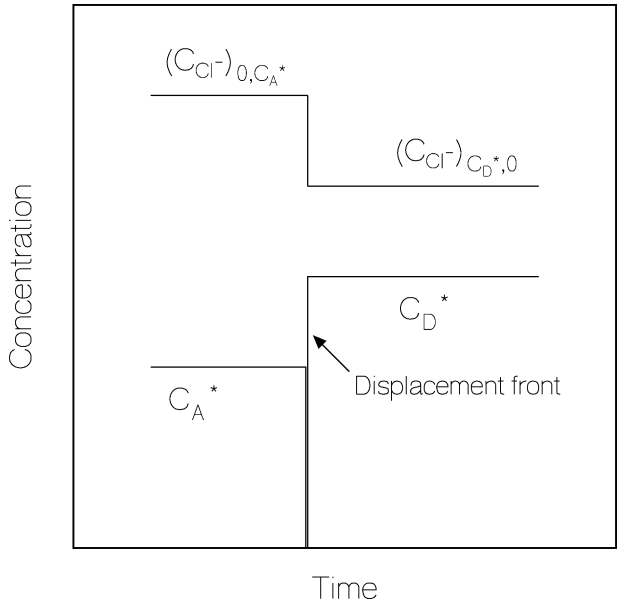

Fig. 2. Concentration profiles for protein A, displacer D, and the counterion Cl^- on the upstream and downstream plateaus of a displacement front. The front is formed by a displacer with a fixed charge as it displaces a protein.

of $n_{protein} + 1$ equations which implicitly define the multicomponent adsorption isotherms. Similarly, for the case of a weak-base anion-exchange adsorbent Eqs. (21) and (24) provide an analogous system of equations that implicitly define the multicomponent adsorption isotherms.

2.6. Theoretical stability criterion for a self-sharpening front between a displacer and a protein

One use of the adsorption isotherm model developed in Section 2.5 is to develop a criterion for determining whether a species of fixed charge is able to displace a protein in displacement chromatography, as illustrated in Fig. 2. Such a criterion, based on a stability analysis originally described by Antia and Horváth [27], has been described previously by Brooks and Cramer [6]. However, the criterion of Brooks and Cramer assumes that the protein being displaced also has a fixed charge as it interacts with the adsorbent, so that it may not be an adequate description of the displacement process for the case where charge regulation is important, such as when the fluid pH is near the p*I* of the displaced protein. For this particular case, which may be of practical importance when it is desired to resolve proteins of similar p*I* values by employing displacement chromatography at a pH near the protein p*I* [28], a modified stability criterion which includes charge regulation effects may be applicable.

Consider the case where a displacer "D" is used to displace protein "A" in the presence of salt under mass overloading conditions, in which case the elution order is "A" followed by "D". For convenience, Eq. (24) applied to protein A is rewritten as

$$\left(\frac{q_A}{C_A}\right) = K_{eq,A}[\exp(\phi')]^{m_A}\Pi(\phi') \tag{25}$$

where Π is a function of ϕ' corresponding to the expression in square brackets in Eq. (24), with the other variables in that expression, such as pH and p*I*, considered to be function parameters. If it is assumed that the displacer is a small molecule with a fixed charge, an example being the protected amino acids described by Kundu et al. [29], then the adsorption distribution coefficient for the displacer can be expressed as

$$\left(\frac{q_D}{C_D}\right) = K_{eq,D}[\exp(\phi')]^{m_D} \tag{26}$$

where $m_D > 0$. In Eq. (26) the effective dimensionless Donnan potential when both protein A and displacer D are present can be expressed as:

$$\phi' = \ln\left(\frac{q_{R^+} - \sigma_A q_A - m_D q_D}{C_{Cl^-}}\right) \tag{27}$$

Consider first the plateau in the displacement chromatography effluent profile which contains the displacer but not the protein, i.e., where $C_A = 0$, $C_D = C_D^*$ and $C_{Cl^-} = (C_{Cl^-})_{C_{D,0}^*}$, and where the superscript * denotes a particular value of C_D. In this case, Eq. (27) yields:

$$\phi'_{C_D^*,0} = \ln\left(\frac{q_{R^+} - m_D q_D}{(C_{Cl^-})_{C_D^*,0}}\right) \tag{28}$$

A necessary criterion for the existence of a stable self-sharpening front separating the plateaus containing the displacer and protein is that the distribution coefficient of a trace amount of protein on the former plateau is less than the distribution coefficient of the displacer on the latter plateau, i.e.,

$$\left(\frac{q_A}{C_A}\right)_{C_D^*,0} = K_{eq,A}[\exp(\phi'_{C_D^*,0})]^{m_A}\Pi(\phi'_{C_D^*,0}) < \delta \tag{29}$$

where

$$\delta \equiv \left(\frac{q_D}{C_D}\right) = K_{D,ads}[\exp(\phi'_{C_D^*,0})]^{m_D} \tag{30}$$

Combining Eqs. (29) and (30) yields:

$$\left(\frac{K_{eq,D}}{\delta}\right)^{1/m_D} > \left[\frac{K_{eq,A}\Pi(\phi'_{C_D^*,0})}{\delta}\right]^{1/m_A} \tag{31}$$

A development similar to that which led to Eqs. (28)–(31), but which applies to the plateau in the effluent profile containing protein but no displacer, i.e., where $C_D = 0$, $C_A = C_A^*$, and $C_{Cl^-} = (C_{Cl^-})_{0,C_A^*}$, yields

$$\phi'_{0,C_A^*} = \ln\left(\frac{q_{R^+} - \sigma_A q_A}{(C_{Cl^-})_{0,C_A^*}}\right) \tag{32}$$

$$\left(\frac{q_D}{C_D}\right)_{0,C_A^*} = K_{eq,D}[\exp(\phi'_{0,C_A^*})]^{m_D} > \delta \quad (33)$$

$$\left(\frac{q_A}{C_A}\right) = K_{A,ads}[\exp(\phi'_{0,C_A^*})]^{m_D} \Pi(\phi'_{0,C_A^*}) = \delta \quad (34)$$

$$\left(\frac{K_{eq,D}}{\delta}\right)^{1/m_D} > \left[\frac{K_{eq,A}\Pi(\phi'_{0,C_A^*})}{\delta}\right]^{1/m_A} \quad (35)$$

Eqs. (31) and (35) can be used to determine whether a particular species is able to displace a protein in displacement chromatography. Although generally this determination is complicated due to the large number of parameters involved, several simplified illustrative cases can be envisioned. For example, for the case of a low-molecular-weight displacer of fixed charged, the salt concentration on the composition plateau containing the displacer is generally lower than the salt concentration on the composition plateau containing the displaced protein, as illustrated in Fig. 2. By comparing Eqs. (28) and (32), it follows that under these conditions $\phi'_{C_D^*,0} > \phi'_{0,C_A^*}$. In this case, Eq. (31) becomes the sole displacement criterion since, according to Eq. (24), Π is a monotonically increasing function of ϕ'. Furthermore, for the case of a displacer and column packing with fixed charges, $\phi'_{C_D^*,0}$ is determined by the salt and displacer concentrations in the displacer solution, so that the function Π becomes independent of the fluid pH. If the value of the function Π under these conditions is denoted as Π_D, and if the dynamic affinity of the displacer, denoted by λ_D, is defined as [29]

$$\lambda_D = \left(\frac{K_{eq,D}}{\delta}\right)^{1/m_D} \quad (36)$$

then the condition needed for displacer D to displace protein A under the assumptions just discussed can be written as

$$\log(K_{eq,A}) < z_{A,fluid}\ \log(\lambda_D) + \log(\delta) + [(m_A - z_{A,fluid})\log(\lambda_D) + \log(\Pi_D)] \quad (37)$$

Note that in Eq. (37) the product $z_{A,fluid}\log(\lambda_D)$ has been added to and subtracted from the right side so that the final form of the relation is analogous to that developed by Brooks and Cramer [6], but with a correction factor for charge regulation given by the quantity in square brackets. An illustration of the use of Eq. (37) is described below in Section 3.4.

3. Results and discussion

3.1. Effect of charge regulation on the SMA model calculations

In order to illustrate the effect of charge regulation on SMA equilibrium for the ion-exchange adsorption of proteins, adsorption isotherms were calculated using two versions of the SMA model: one being the traditional SMA model developed by Brooks and Cramer [6] where charge regulation is ignored; the other being the extension of the traditional SMA model to the case where charge regulation is included. The results of these calculations are shown in Fig. 3. Note that the calculations shown employ physical properties representative of bovine serum albumin (BSA) adsorption onto an anion-exchange column packing, as discussed in Section 3.3. In addition, the parameter m, which is the maximum charge of the protein, is set at two times the minimum possible value of $\sqrt{-3(dz/dpH)_{pI}/(2\ \ln(10))}$, as discussed by Shen and Frey [15], and the characteristic binding charge used in the version of the SMA model ignoring charge regulation was assumed to be the average charge of all the charged forms of the protein in the fluid phase. The calculations also employed a fluid-phase pH of 5.0, which is 0.2 pH units above the protein pI so that protein binding occurred onto the anion-exchange adsorbent assumed in the calculations even in the absence of charge regulation.

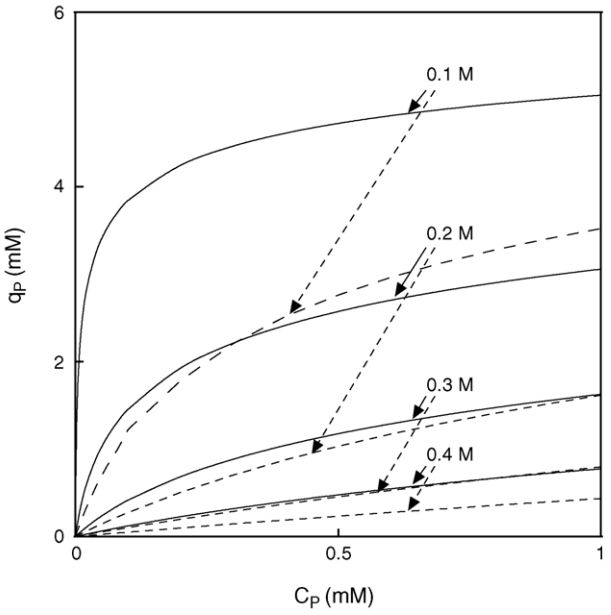

Fig. 3. Comparison of adsorption isotherms calculated from SMA models with (solid curve) and without (dotted curve) consideration of charge regulation. The numbers in the figure denote the ionic strengths used for the calculations. The physical properties used for the protein and column packing are as follows: pI = 4.8, $(dz/dpH)_{pI} = -10$, $\sigma = 100$, $m = 5.1$, $K_{eq,P} = 0.1$, $q_R = 0.75$ M. The fluid-phase pH is 5.0.

The results in Fig. 3 illustrate that including the effect of charge regulation in the SMA model for a given protein charge in the fluid phase causes a significant increase in the amount adsorbed, especially at low salt and protein concentrations. These trends are not unexpected since charge regulation becomes predominant at low salt concentration due to the fact that the Donnan potential becomes higher in this region, while at high protein concentrations the amount adsorbed is determined by the steric factor regardless of whether charge regulation is accounted for. The relatively large discrepancy between the two models shown in Fig. 3 indicates that, apart from other effects such as charge asymmetry which cause the

characteristic binding charge to differ from the true protein charge, the use of the true fluid-phase charge in the traditional version of the SMA model which ignores charge regulation is unlikely to fit experimental data accurately. Instead, when the traditional SMA model is fitted to experimental data, the fitted characteristic protein charge is to a large extent an effective average charge for the protein considering both the fluid and adsorbed phases. This effective charge is likely to differ significantly from the true fluid-phase protein charge, especially when the fluid-phase pH and protein p*I* are close in value. In particular, in order to raise the curve shown in Fig. 3 for the traditional SMA model at 0.1 M NaCl so that it overlies the corresponding result from the model including charge regulation, a fixed charge of −4.5 is needed in the former SMA model. This can be compared to the average protein charge in the fluid phase of −2.6, and the average protein charge in the adsorbed phases of −5.1, that apply to the MCS model used in the figure.

3.2. Effect of pH

The fluid-phase salt concentration and pH typically are the most important parameters which determine the adsorption affinity of a protein in ion-exchange chromatography. The effect of salt concentration has been extensively studied and explicitly incorporated into many ion-exchange models [5,6,17,18,30,31]. However, previous descriptions in the literature of the effect of pH on the adsorption affinity of proteins under mass-overloaded conditions have been limited to qualitative [32] or semi-quantitative studies [4], all of which ignore the effects of charge regulation. In contrast, in the present work as represented by Eq. (22), the effect of pH is incorporated by assuming that the Henderson–Hasselbalch equation applies to three charged forms of a protein in equilibrium, by then relating the acid–base equilibrium constants to the values of p*I* and $(dz/dpH)_{pI}$ for the protein, and by finally assuming that the SMA formalism, as represented by the Boltzmann distributions given by Eqs. (7)–(9), applies to each charged form of the protein [15]. In this way the role of pH variations, particularly when the pH is near the protein p*I*, can be realistically incorporated into calculations of adsorption equilibrium.

Fig. 4 illustrates calculations of protein adsorption equilibrium for the case of an anion-exchange column packing using the SMA model with the effects of charge regulation accounted for as just discussed. The physical properties of the protein and column packing used in the calculations are the same as those in Fig. 3 and are representative of BSA adsorption onto an anion-exchange column packing. Two notable features can be observed in the calculations shown. First, it is apparent that the adsorption affinity is highly dependent on the fluid-phase pH, and that this dependence tends to be greater than that produced by changes in the salt concentration as shown in Fig. 3. Second, the model predicts that highly favorable shapes for the adsorption isotherm, i.e., high-affinity protein binding, occur in the region where the

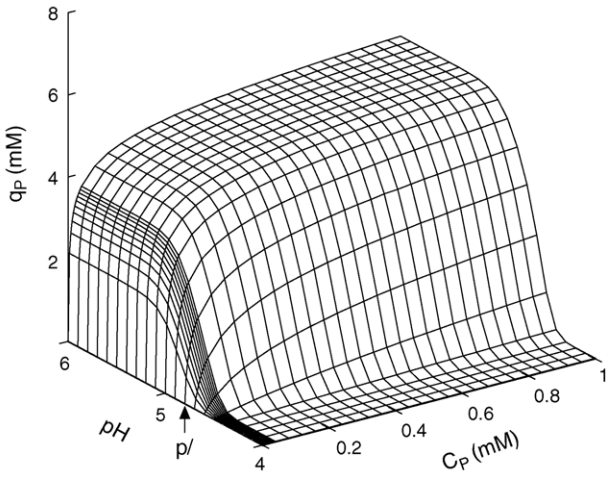

Fig. 4. The theoretically calculated protein concentration in the adsorbed phase as a function of the fluid-phase protein concentration and pH. The physical properties used for the protein and column packing are the same as in Fig. 3. The ionic strength is 0.1 M. The grid lines parallel to the pH axis between $C_p = 0$ and $C_p = 0.04$ M have one tenth the spacing distance as compared to the remainder of these types of grid lines in order to better illustrate the steepness of the isotherm surface in this range.

pH in the fluid phase is equivalent to, or even lower than, the protein p*I*. High affinity binding of this type is further demonstrated experimentally in Section 3.3. In contrast, without the effects of charge regulation included, adsorption isotherms predicted by the SMA model tend to be linear in nature when the protein charge in the fluid phase is small and if this charge is used to predict the adsorption affinity.

The observations just described suggest that the SMA model incorporating the effects of charge regulation may provide a more accurate description of adsorption equilibrium as compared to the standard SMA model when the pH in the fluid phase is close to the protein p*I*. This may be particularly important in the design and optimization of preparative-scale chromatographic processes since it has been reported that the separation of proteins under mass-overloaded conditions, including for the case where displacement chromatography is employed, can be enhanced if the fluid-phase pH is adjusted so that it is close to the protein p*I* [28,33,34].

3.3. Evaluation of the SMA model including the effects of charge regulation using data from the literature

The SMA model which includes the effects of charge regulation as developed in this study was evaluated using experimental data reported by Shi et al. [35] for the adsorption of BSA on DEAE Sepharose FF, which is a weak-base anion-exchange column packing. The comparison between the model and the experimental data is illustrated in Figs. 5–8 where the adsorbed amounts shown are given in terms of the mass of BSA per unit volume of solid adsorbent, and where the solid adsorbent volume does not include the intraparticle pores. Since the data of Shi et al. are given in terms of the mass of BSA per unit volume of particle, where the particle

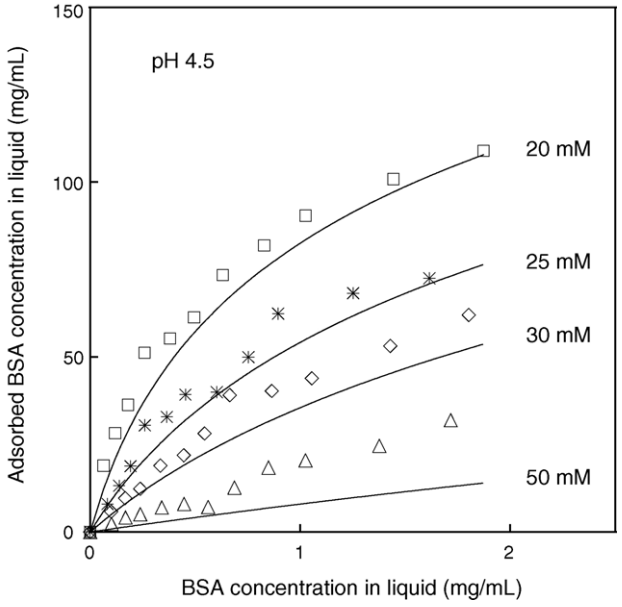

Fig. 5. Comparison of experimentally measured and theoretically predicted adsorption isotherms for BSA on DEAE Sepharose FF. The symbols are data from batch equilibrium experiments taken from the literature and the solid curves are calculated results from the SMA model with charge regulation considered. The fluid-phase pH is 4.5 and the physical properties used for the protein and column packing are as follows: MW = 66.7 kDa, pI = 4.7, $(dz/dpH)_{pI} = -10$, $\sigma = 98$, $m = 3.6$, $K_{P,ads} = 0.17$, $q_R = 0.51$ M. In the experiments, the fluid phase contained 20 mM acetate buffer at various ionic strengths as represented by the following symbols: 20 mM (□); 25 mM (✳); 30 mM (◊); 50 mM (△). The temperature was 25 °C.

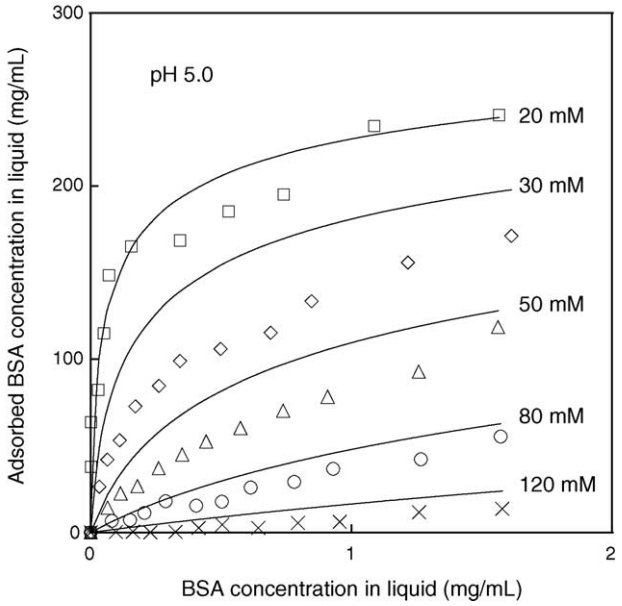

Fig. 6. Comparison of experimentally measured and theoretically predicted adsorption isotherms for BSA on DEAE Sepharose FF. The symbols are data from batch equilibrium experiments taken from the literature and the solid curves are calculated results from the SMA model with charge regulation considered. The fluid-phase pH is 5.0 and the physical properties used for the protein and column packing are the same as in Fig. 5. In the experiments, the fluid phase contained 20 mM acetate buffer at various ionic strengths as represented by the following symbols: 20 mM (□); 30 mM (◊); 50 mM (△); 80 mM (◯); 120 mM (×). The temperature was 25 °C.

volume does include the intraparticle pores, it was necessary to convert this data by using the reported particle porosity of 0.59 [36]. Note also that the data shown were obtained under conditions where the fluid-phase pH is close to the protein pI, so that these data are particularly useful for evaluating the model described here. However, the specific data obtained by Shi et al. at pH 6 was not utilized when evaluating the model since it was judged that this condition was outside the applicable range of the model due to the high charge attained by BSA at this pH. The experimental conditions and the physical properties used in the calculations are described further in the figure captions.

In order to fit the experimental data to the model, all the data sets were fitted simultaneously using a single set of physical properties for BSA. The fitting was accomplished by calculating the amount adsorbed as described previously while simultaneously minimizing the sum of the squared residuals between the measured and calculated amount adsorbed. For this purpose, the concentration of the functional groups on the column packing was taken to be that specified by the column manufacturer [37], and a pK_R value of 8 was assumed, which is typical for the diethylaminoethyl (DEAE) groups present. Using this procedure, in the pH range of interest the functional groups on the column packing were nearly completely ionized, and the calculated change in q_{R^+} with pH was relatively small and roughly agreed with the reported

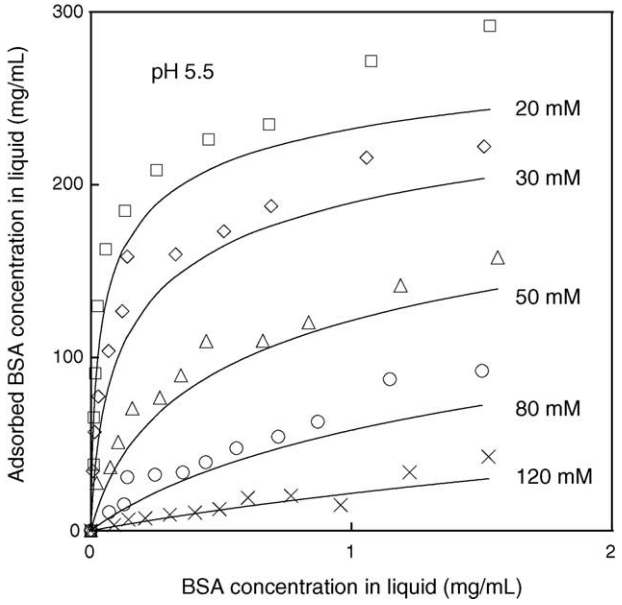

Fig. 7. Comparison of experimentally measured and theoretically predicted adsorption isotherms for BSA on DEAE Sepharose FF. The symbols are data from batch equilibrium experiments taken from the literature and the solid curves are calculated results from the SMA model with charge regulation considered. The fluid-phase pH is 5.5 and the physical properties used for the protein and column packing are the same as in Fig. 5. In the experiments, the fluid phase contained 20 mM acetate buffer at various ionic strengths as represented by the following symbols: 20 mM (□); 30 mM (◊); 50 mM (△); 80 mM (◯); 120 mM (×). The temperature was 25 °C.

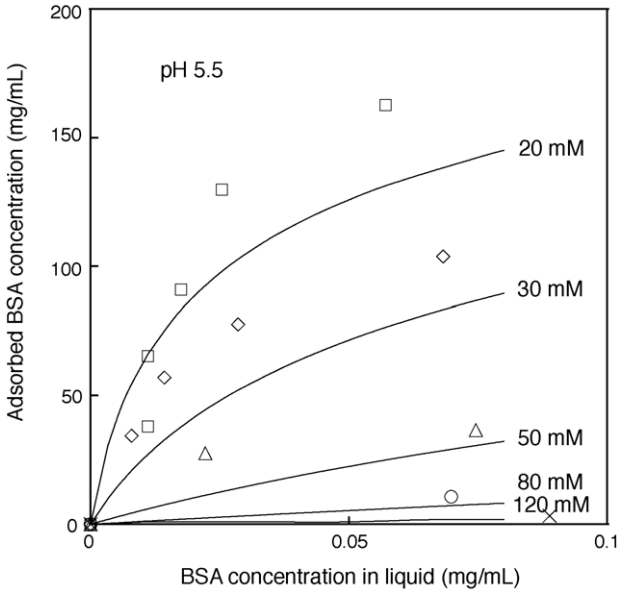

Fig. 8. Expanded view taken from Fig. 7 of the isotherms for the adsorption of BSA on DEAE Sepharose FF in the low concentration region.

titration curve [38] and the zeta potential measurements [39] for DEAE Sepharose FF. To simplify the calculations, a single counterion having an average adsorption affinity was assumed even though the fluid phase employed to produce the data consisted of a mixture of acetate and chloride ions due to the acetate buffer used. In addition, the salt concentrations that apply at pH 4.5 were assumed to be those shown at this pH in Fig. 4 of Shi et al. [35].

As shown in Figs. 5–8, the model is able to fit the experimental data reasonably well using physical properties which are representative of the protein and column packing used. In particular, the assumed value of $(dz/dpH)_{pI}$ of -10 is near the reported value for this parameter for human serum albumin [40], the fitted p*I* of 4.7 is near the actual p*I* of BSA, which is reported to lie in the range from 4.7 to 5.18 [17,35,41,42], the fitted value of m of 3.6 is slightly larger than the minimum possible value of $\sqrt{-3(dz/dpH)_{pI}/(2\ \ln(10))}$, as discussed by Shen and Frey [15], and the fitted values of σ and $K_{eq,P}$ for the DEAE Sepharose FF column packing used are comparable to values reported in previous studies [15,17,18,35].

Although the model was able to fit experimental adsorption data reasonably well for the weak-base anion-exchange adsorbent used as just mentioned, past work [15] indicates that the MCS model tends to be more suitable for a strong-base anion-exchange adsorbent since the value of q_{R^+} is directly specified in this case. The good agreement between theory and experiments in Figs. 5–8 is therefore to some extent due to the low pH range used which caused the adsorbent functional groups to be nearly completely ionized.

One main observation from Figs. 5–8 is that the amount of BSA adsorbed when the pH is near or below the p*I* of BSA is accounted for reasonably well by the mechanism of charge regulation. This is in contrast to the conclusions of Shi et al. [35] who proposed that adsorption under these conditions results mainly from the presence of localized regions of negative charge on the BSA surface, i.e., from charge asymmetry. In all likelihood, both charge asymmetry and charge regulation play a role in determining the amount of BSA adsorbed, although the results presented here suggest that the latter mechanism may dominate for the particular conditions investigated. Another observation from Figs. 5–8 is that a single value for the steric factor is able to fit with reasonable accuracy the BSA adsorption data obtained on both sides of the p*I*. This observation is also in contrast to the conclusions of Shi et al. who used the traditional SMA model and found that the steric factors for BSA needed to fit data obtained above and below the p*I* were somewhat different. This discrepancy in the parameters needed by the two models to fit the same data is due in part to the somewhat different functional form that results for the adsorption isotherm when charge regulation is incorporated into the SMA model. In addition, in the present study the volume of solid adsorbent, instead of the volume of particle, was used as the basis for determining the adsorbed protein concentration. By employing this former choice, the value of $K_{eq,P}$ used to fit the data became nearly independent of pH and ionic strength, rather than varying significantly with these conditions as in the study of Shi et al., which in turn affected the values of the other parameters needed by the two models to fit the data. Finally, differences in how the weak-base character of the adsorbent was accounted for may have also contributed to discrepancies in how the two models fit data.

It should also be noted that the relatively small values of $K_{eq,P}$ used in Figs. 5–8 are consistent with the observation of Nagai and Carta [26] that the zwitterion form of an amino acid is largely unadsorbed by most typical ion-exchange adsorbents, since the value of $K_{eq,P}$ directly determines the amount of the uncharged form adsorbed. Finally, since the data in Fig. 8 is an expanded view at low protein concentrations of the data in Fig. 7, it can be seen that the model calculations agree with the data over a large protein concentration range which includes low concentrations where linear equilibrium applies.

3.4. Stability analysis for a self-sharpening front located between a displacer and a displaced protein

Section 2.6 describes a stability criterion for a self-sharpening front located between a displacer and a displaced protein based on the SMA model with charge regulation considered. In this section, this stability criterion is used to produce a so-called dynamic affinity plot describing the relation needed between a low-molecular-weight displacer with a fixed charge and a displaced protein with the value of $(dz/dpH)_{pI}$ for the protein as a parameter. A typical plot of this type is shown in Fig. 9 with the physical properties for the protein, displacer, salt, and column packing used in the calculations listed in the figure caption. The solid curves in the figure were calculated from Eq. (37) by setting the quantity on the left-hand side of that equation equal to that

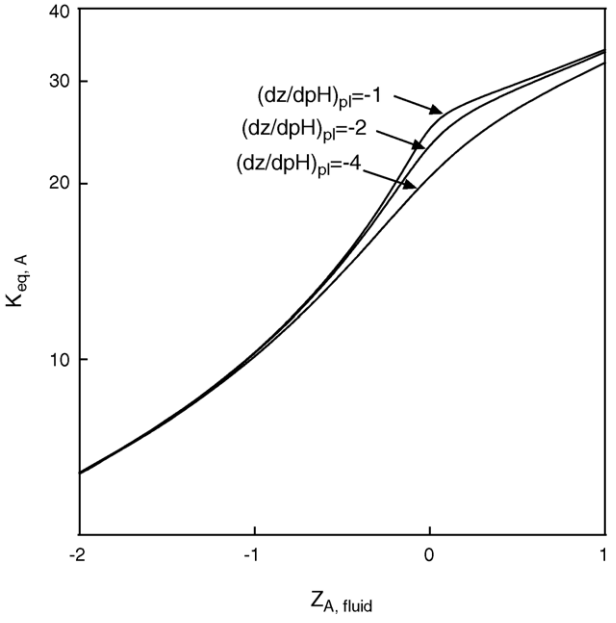

Fig. 9. Dynamic affinity plot for a displacer and a protein for an anion-exchange column packing. The solid curves are the calculated results at different values of $(dz/dpH)_{pI}$ for the protein. The physical properties for the protein, displacer, and column packing are as follows: pI = 6, m_A = 4, m_D = 1, $K_{eq,D}$ = 50.0, δ = 120, ϕ' = 0.5.

on the right-hand side. The curves therefore divide the figure into two regions: a lower region where a protein will be displaced by the given displacer, and a higher region where a protein will not be displaced by the given displacer. Note that the calculations shown correspond to an anion-exchange column packing, that $z_{A,fluid}$ is the average charge considering all the charged forms of the protein in the fluid phase, and that the calculations are for a particular fixed value of the effective dimensionless Donnan potential in the displacer solution as discussed in Section 2.6.

Fig. 9 indicates that the dynamic affinity plots accounting for charge regulation are curved, with the maximum in curvature close to the protein pI, and with the degree of the curvature dependent on the value of $(dz/dpH)_{pI}$. This is in contrast to the linear dynamic affinity plots described by Brooks and Cramer where charge regulation is ignored [6]. As also shown in the figure, the higher the value of $(dz/dpH)_{pI}$ for the protein, the lower the position of the dynamic affinity curve. This suggests that it is harder to displace a protein with a higher value of $(dz/dpH)_{pI}$, in which case this parameter may play an important role in displacement chromatography, especially when the pH in the fluid phase is close to the protein pI. Another feature of Fig. 9 is that the dynamic affinity plot provides a displacement criterion for a displacer and protein combination when the protein in the fluid phase is uncharged or even the same charge sign as the column packing. This again contrasts with the stability analysis developed by Brook and Cramer based on the traditional SMA model where linear adsorption equilibrium applies when the fluid-phase protein is uncharged, in which case displacement effects are not possible, and where protein binding is largely absent when the protein in the fluid phase and column packing have the same charge sign, so that again displacement effects are not possible.

Although, as discussed in Section 3.1, when used in practice the traditional SMA model incorporates an effective average of the protein charge in the fluid and adsorbed phases so that the associated dynamic affinity plot accounts approximately for the case when the protein and column packing have the same charge sign, it seems evident that the representation of adsorption behavior shown in Fig. 9 provides a more fundamental and therefore more accurate description of the adsorption behavior when the pH is near the protein pI. The importance of this is suggested by the observation that the resolution achieved between β-lactoglobulin A and B in displacement chromatography is enhanced when the fluid-phase pH used approaches the protein pI [28], so that it may be true generally that resolution in displacement chromatography is optimized under these types of conditions. In addition, for the type of displacement chromatography where a self-sharpening pH front is employed as the displacer, displaced proteins always exit the column at a pH close to the protein pI so that accounting for charge regulation is likely to be an important factor in the understanding of such systems [43]. In contrast, when the pH and protein pI are far apart, charge regulation is likely to be unimportant. In this case the traditional SMA model and the dynamic affinity plot derived from that model are likely to be the preferred representations of adsorption dynamics, especially since the model for charge regulation described in this study is not expected to apply when the pH and protein pI are far apart.

4. Conclusions

The concept of steric mass-action equilibrium for protein ion-exchange adsorption equilibrium was originated by Velayudhan [19], and was first put into precise mathematical terms by Brooks and Cramer [6]. The basic assumptions of the SMA model proposed by Brooks and Cramer are that, with regard to their role in protein adsorption equilibrium, sterically hindered adsorption sites located underneath an adsorbed protein function thermodynamically as if the counterions and the adsorption sites are undissociated ion pairs and that, due to the diffusional mobility of adsorbed proteins, the activity of exchangeable counterions is proportional to the number of these ions per unit volume of the total adsorbed phase, including the volume occupied by the sterically hindered sites. Although the formalism of Brooks and Cramer is by no means the only method which could be used to account for the effects of sterically hindered counterions on protein adsorption, many studies over the last several years indicate that it is a reasonably realistic depiction of protein adsorption behavior [29,44–52]

In the present work, a logical extension of the SMA model of Brooks and Cramer [6] is proposed which accounts for the

effect of the change in protein charge caused by electrostatic interactions between the protein and the adsorbent surface, i.e., the effects of charge regulation. This extension is accomplished by accounting for the existence of multiple protein charge states when formulating the SMA adsorption equilibrium expressions. The result is a new protein adsorption model which applies to the case of mass overloading and which is extension of the original SMA model of Brooks and Cramer to the case where charge regulation is important. The new model is also an extension of the charge regulation model for dilute proteins of Shen and Frey [15], since it reduces to the latter model for the case of low protein concentrations.

Comparisons of calculations using the new model and experimental data for protein ion-exchange adsorption indicate that the model fits the data with acceptable accuracy when using reasonable physical properties, including reasonable values for the protein pI and for the change in protein charge with pH near the protein pI, i.e. $(\mathrm{dz/dpH})_{\mathrm{p}I}$. The results therefore indicate that when charge regulation is accounted for in the SMA model, the fluid-phase protein charge used in the model is much closer to the actual charge of the protein in the fluid phase, as compared to when the traditional SMA model is used. Similar results for dilute proteins where linear adsorption equilibrium applies were also observed by Shen and Frey [15].

The new model developed here also leads to additional insights into the dynamics of protein adsorption in nonlinear chromatography, including a new version of the dynamic affinity plot describing the process of displacement chromatography where the dynamic affinity contours are nonlinear and incorporate the quantity $(\mathrm{dz/dpH})_{\mathrm{p}I}$ as a parameter. Finally, the new model is expected to be particularly useful for representing nonlinear ion-exchange adsorption equilibrium for proteins when the fluid-phase pH is near the protein pI — which is an operating region proposed by some workers for enhancing the resolution in displacement chromatography [28].

Despite the good agreement between experimental data and the calculations from the model shown in Figs. 5–8, it is possible that in certain cases various phenomena not currently included in the model may lead to significant differences between the fluid-phase charge needed to fit adsorption data using the model and the actual protein charge in the fluid phase. Examples of such phenomena include the nonuniform nature of the electric potential near the adsorbent surface, charge asymmetry on the protein surface which varies with pH, and structural changes in the protein caused by adsorption. Nevertheless, even in cases where these other phenomena dominate the effects of charge regulation, the model presented in this study may still be useful as a means to quantitatively account for charge regulation so these more dominant effects can be more easily identified.

Note finally that the parameters $-m$ and m introduced in Section 2.3 have been interpreted as the net charge states of the entire protein due to the fact that when the pH is near the protein pI, Eq. (22) often fits protein adsorption data using values for the pI and $(\mathrm{dz/dpH})_{\mathrm{p}I}$ in that equation that are near the values reported for the entire protein in free solution [15]. However, in cases where ion-exchange adsorption is considered to be determined by a single localized charge region on the protein surface, the model developed here may still be applicable by reinterpreting these various parameters to be those that apply to the surface region in question.

5. Nomenclature

C_{A}	concentration of protein A in the fluid phase (mol/L)
C_{Cl^-}	concentration of Cl^- in the fluid phase (mol/L)
$(C_{\mathrm{Cl}^-})_{0,C^*_{\mathrm{A}}}$	concentration of Cl^- in the fluid phase when $C_{\mathrm{D}} = 0$ and $C_{\mathrm{A}} = C^*_{\mathrm{A}}$ (mol/L)
$(C_{\mathrm{Cl}^-})_{C^*_{\mathrm{D}},0}$	concentration of Cl^- in the fluid phase when $C_{\mathrm{A}} = 0$ and $C_{\mathrm{D}} = C^*_{\mathrm{D}}$ (mol/L)
C_{D}	concentration of displacer D in the fluid phase (mol/L)
C_{H^+}	concentration of H^+ in the fluid phase (mol/L)
$C_{i,j}$	concentration of the jth charge state of protein i in the fluid phase (mol/L)
C_{P^z}	concentration of a protein charge form in the fluid phase where z is $-m$, 0, or m (mol/L)
i	index for protein
j	index for charge state
$K_{\mathrm{Cl}^-,\mathrm{ads}}$	adsorption equilibrium constant for Cl^-
K_{d}	distribution coefficient
$K_{\mathrm{eq,A}}$	adsorption equilibrium constant for protein A
$K_{\mathrm{eq,D}}$	adsorption equilibrium constant of displacer D
$K_{\mathrm{eq},i}$	adsorption equilibrium constant of protein i
$K_{\mathrm{eq,P}}$	adsorption equilibrium constant which is equivalent to the quantity $K_{\mathrm{P,ads}}/(K^{-z}_{\mathrm{Cl}^-,\mathrm{ads}})$ where z is $-m$, 0, or m
$K_{\mathrm{P,ads}}$	adsorption equilibrium constant of protein
K_{R}	dissociation constant for the functional group on the column packing
m	parameter used in the MCS model where $n = 2m + 1$
m_{D}	fixed charge of displacer D
m_i	maximum charge on protein i
n	total number of charge states for a protein that exist between the $-m$ and m charge states
n_{protein}	number of proteins present
pI	isoelectric point of a protein
q_{A}	concentration of protein A in the adsorbed phase (mol/L)
q_{Cl^-}	concentration of Cl^- in the adsorbed phase (mol/L)
$q_{\mathrm{Cl}^-,\mathrm{a}}$	the amount of exchangeable counterion per unit volume of the adsorbed phase (mol/L)
q_{D}	concentration of displacer D in the adsorbed phase (mol/L)
$q_{i,j}$	concentration of the jth charge state of protein i in the adsorbed phase (mol/L)
q_{P}	total concentration of protein considering all charge forms in the adsorbed phase (mol/L)

q_{P^z} concentration of a protein in the z charge state in the adsorbed phase where z is $-m$, 0, or m (mol/L)
q_R total concentration of the ionogenic functional group on the column packing (mol/L)
q_{R^+} concentration of the charged form of the ionogenic functional group on the column packing (mol/L)
z charge on each form of the protein
z_{ave} average charge for a mixture of proteins in the adsorbed phase
$z_{A,fluid}$ average charge on protein A in the fluid phase
$z_{i,j}$ jth charge state of protein i

Greek letters

δ distribution coefficient for the displacer
λ_D dynamic affinity of the displacer
Π function of the effective dimensionless Donnan potential defined by the expression in square brackets in Eq. (22)
Π_D value of Π for a displacer solution containing displacer having a fixed charge
σ total number of adsorption sites underneath a protein
σ_A total number of adsorption sites underneath protein A
σ_{BC} steric factor for the protein in the Brooks and Cramer model, $\sigma_{BC} = \sigma - m$
σ_i total number of adsorption sites underneath protein i
ϕ dimensionless Donnan potential, equivalent to $\ln(q_{Cl^-}/C_{Cl^-})$
ϕ' effective dimensionless Donnan potential, equivalent to $\ln(q_{Cl^-,a}/C_{Cl^-})$
ϕ'_{0,C^*_A} effective dimensionless Donnan potential when $C_D = 0$ and $C_A = C^*_A$
$\phi'_{C^*_D,0}$ effective dimensionless Donnan potential when $C_A = 0$ and $C_D = C^*_D$

Superscript

$'$ effective value based on $q_{Cl^-,a}$ instead of q_{Cl^-}

Acknowledgement

Support from grants CTS 9813658 and CTS 0442072 from the National Science Foundation is greatly appreciated. We thank Dr. Yan Sun at Tianjin University for supplying the data from reference 35 in tabular form.

References

[1] N.K. Boardman, S.M. Partridge, Biochem. J. 59 (1955) 543.
[2] J. Ståhlberg, B. Jönsson, Cs. Horváth, Anal. Chem. 63 (1991) 1867.
[3] C.M. Roth, K.K. Unger, A.M. Lenhoff, J. Chromatogr. A 726 (1996) 45.
[4] A. Velayudhan, Cs. Horváth, J. Chromatogr. 367 (1986) 160.
[5] P. Cysewski, A. Jaulmes, R. Lemque, B. Sebille, C. Vidal-Madjar, G. Jilge, J. Chromatogr. 548 (1991) 61.
[6] C.A. Brooks, S.M. Cramer, AIChE J. 38 (1992) 1969.
[7] P. Raje, N.G. Pinto, J. Chromatogr. A 760 (1997) 89.
[8] S.H. Behrens, M. Borkovec, J. Chem. Phys. 111 (1999) 382.
[9] D. Chan, J.W. Perram, L.R. White, T.W. Healy, J. Chem. Soc., Faraday Trans. I 71 (1975) 1046.
[10] S.L. Carnie, D.Y.C. Chan, J.S. Gunning, Langmuir 10 (1994) 2993.
[11] S.H. Behrens, D.G. Grier, J. Chem. Phys. 115 (2001) 6716.
[12] B.W. Ninham, V.A. Parsegian, J. Theor. Biol. 31 (1971) 405.
[13] L.A.A. Sluyterman, O. Elgersma, J. Chromatogr. 150 (1978) 17.
[14] J. Ståhlberg, B. Jönsson, Anal. Chem. 68 (1996) 1536.
[15] H. Shen, D.D. Frey, J. Chromatogr. A 1034 (2004) 55.
[16] P. Raje, N.G. Pinto, J. Chromatogr. A 796 (1998) 141.
[17] J.C. Bosma, J.A. Wesselingh, AIChE J. 44 (1998) 2399.
[18] J.C. Bosma, J.A. Wesselingh, AIChE J. 50 (2004) 887.
[19] A. Velayudhan, Ph.D. Thesis, Yale University, New Haven, CT, 1990.
[20] J.T.G. Overbeek, Progr. Biophys. Biophys. Chem. 6 (1956) 57.
[21] J.S. Newman, Electrochemical Systems, Prentice-Hall, Englewood Cliffs, NJ, 1973.
[22] P.-A. Albertsson, Partition of Cell Particles and Macromolecules, Wiley Interscience, New York, NY, 1986.
[23] C.A. Haynes, J. Carson, H.W. Blanch, J.M. Prausnitz, AIChE J. 37 (1991) 1401.
[24] A.P. Sassi, H.W. Blanch, J.M. Prausnitz, AIChE J. 42 (1996) 2335.
[25] J.M. Prausnitz, R.N. Lichtenthaler, E.G. de Azevedo, Molecular Thermodynamics of Fluid-Phase Equilibria, Prentice-Hall PTR, Upper Saddle River, NJ, 1999.
[26] H. Nagai, G. Carta, Sep. Sci. Technol. 39 (2004) 3691.
[27] F.D. Antia, Cs. Horváth, J. Chromatogr. 556 (1991) 119.
[28] G. Chen, W.H. Scouten, J. Mol. Recogn. 9 (1996) 415.
[29] A. Kundu, S. Vunnum, G. Jayaraman, S.M. Cramer, Biotech. Bioeng. 48 (1995) 452.
[30] A. Velayudhan, Cs. Horváth, J. Chromatogr. 443 (1988) 13.
[31] Y. Li, N.G. Pinto, J. Chromatogr. A 702 (1995) 113.
[32] C.J.O.R. Morris, P. Morris, Separation Methods in Biochemistry, Wiley, New York, NY, 1976.
[33] S. Yamamoto, T. Ishihara, J. Chromatogr. A 852 (1999) 31.
[34] Y.-B. Yang, K. Harrison, J. Chromatogr. A 743 (1996) 171.
[35] Q. Shi, Y. Zhou, Y. Sun, Biotech. Prog. (2005) in press.
[36] S.P. Zhang, Y. Sun, AIChE J. 48 (2002) 178.
[37] Biodirectory '99 Product Catalog, Amersham Pharmacia Biotech, Uppsala, 1999.
[38] Amersham Biosciences, Ion Exchange Chromatography and Chromatofocusing, Amersham, Uppsala, 2004.
[39] D.-Q. Lin, P.J. Brixius, J.J. Hubbuch, J. Thömmes, M.-R. Kula, Biotech. Bioeng 83 (2003) 149.
[40] C. Tanford, J. Am. Chem. Soc. 72 (1950) 441.
[41] P.G. Righetti, T. Caravaggio, J. Chromatogr. 127 (1976) 1.
[42] D. Malamud, J.W. Drysdale, Anal. Biochem. 86 (1978) 620.
[43] C.R. Narahari, J.C. Strong, D.D. Frey, J. Chromatogr. A 825 (1998) 115.
[44] S.R. Gallant, A. Kundu, S.M. Cramer, J. Chromatogr. A 702 (1995) 125.
[45] S.R. Gallant, A. Kundu, S.M. Cramer, Biotech. Bioeng. 47 (1995) 355.
[46] A. Kundu, K.A. Barnthouse, S.M. Cramer, Biotech. Bioeng. 56 (1997) 119.
[47] H. Iyer, S. Tapper, P. Lester, B. Wolk, R. van Reis, J. Chromatogr. A 832 (1999) 1.
[48] V. Natarajan, S.M. Cramer, Sep. Sci. Technol. 35 (2000) 1719.
[49] V. Natarajan, B.W. Bequette, S.M. Cramer, J. Chromatogr. A 876 (2000) 51.
[50] V. Natarajan, S.M. Cramer, J. Chromatogr. A 876 (2000) 63.
[51] S. Ghose, S.M. Cramer, J. Chromatogr. A 928 (2001) 13.
[52] V. Natarajan, S. Ghose, S.M. Cramer, Biotech. Bioeng. 78 (2002) 365.